

Est.  
1841

YORK  
ST JOHN  
UNIVERSITY

Sun, Chuanzhe ORCID logoORCID:  
<https://orcid.org/0000-0003-4405-6391>, Zhong, Jicheng, Pan, Gang  
ORCID logoORCID: <https://orcid.org/0000-0003-0920-3018>,  
Mortimer, Robert ORCID logoORCID: <https://orcid.org/0000-0003-1292-8861>, Yu, Juhua, Wen, Shuailong, Zhang, Lei, Yin, Hongbin  
ORCID logoORCID: <https://orcid.org/0000-0002-7290-2500> and  
Fan, Chengxin (2023) Controlling internal nitrogen and phosphorus  
loading using Ca-poor soil capping in shallow eutrophic lakes:  
Long-term effects and mechanisms. *Water Research*, 233. p.  
119797.

Downloaded from: <https://ray.yorks.ac.uk/id/eprint/7545/>

The version presented here may differ from the published version or version of record. If  
you intend to cite from the work you are advised to consult the publisher's version:  
<http://dx.doi.org/10.1016/j.watres.2023.119797>

Research at York St John (RaY) is an institutional repository. It supports the principles of  
open access by making the research outputs of the University available in digital form.  
Copyright of the items stored in RaY reside with the authors and/or other copyright  
owners. Users may access full text items free of charge, and may download a copy for  
private study or non-commercial research. For further reuse terms, see licence terms  
governing individual outputs. [Institutional Repository Policy Statement](#)

# RaY

Research at the University of York St John

For more information please contact RaY at [ray@yorks.ac.uk](mailto:ray@yorks.ac.uk)

1 Controlling internal nitrogen and phosphorus loading using  
2 Ca-poor soil capping in shallow eutrophic lakes: Long-term  
3 effects and mechanisms

4

5 Chuanzhe Sun<sup>a,e</sup>, Jicheng Zhong<sup>a,\*</sup>, Gang Pan<sup>b,c</sup>, Robert J.G. Mortimer<sup>b</sup>, Juhua Yu<sup>a,d</sup>,  
6 Shuailong Wen<sup>a,e</sup>, Lei Zhang<sup>a</sup>, Hongbin Yin<sup>a</sup>, Chengxin Fan<sup>a</sup>

7

8 <sup>a</sup> State Key Laboratory of Lake Science and Environment, Nanjing Institute of  
9 Geography and Limnology, Chinese Academy of Sciences, Nanjing 210008, PR  
10 China

11 <sup>b</sup> School of Humanities, York St John University, Lord Mayor's Walk, York, YO31  
12 7EX, UK

13 <sup>c</sup> School of Chemical and Environmental Sciences, Guangdong Ocean University,  
14 Zhanjiang 524088, China

15 <sup>d</sup> Institute of Soil and Fertilizer, Fujian Academy of Agricultural Sciences, Fuzhou,  
16 350013, PR China

17 <sup>e</sup> University of Chinese Academy of Sciences, Beijing 100049, PR China

18

19

20 \* Corresponding author:

21 Name: Jicheng Zhong

22 E-mail address: [jczhong@niglas.ac.cn](mailto:jczhong@niglas.ac.cn)

23 Tel: +86-25-86882212; Fax: +86-25-57714759

24

25

26

27

28

29

30

31

32

33 **Abstract**

34 Clean soil is a potential capping material for controlling internal  
35 nutrient loading and helping the recovery of macrophytes in eutrophic  
36 lakes, but the long-term effects and underlying mechanisms of clean soil  
37 capping under in-situ conditions remain poorly understood. In this study, a  
38 three-year field capping enclosure experiment **combining** intact sediment  
39 core incubation, in-situ porewater sampling, isotherm adsorption  
40 experiments and analysis of sediment nitrogen (N) and phosphorus (P)  
41 fractions was conducted to assess the long-term performance of clean soil  
42 capping on internal loading in Lake Taihu. Our results indicate that clean  
43 soil has excellent P adsorption and retention capacity as an ecologically  
44 safe capping material and can effectively mitigate  $\text{NH}_4^+$ -N and SRP  
45 (**soluble reactive P**) fluxes at the sediment-water interface (**SWI**) and  
46 porewater SRP concentration for one year after capping. The mean  $\text{NH}_4^+$ -N  
47 and SRP fluxes of capping sediment were  $34.86 \text{ mg}\cdot\text{m}^{-2}\cdot\text{h}^{-1}$  and  $-1.58$   
48  $\text{mg}\cdot\text{m}^{-2}\cdot\text{h}^{-1}$ , compared  $82.99 \text{ mg}\cdot\text{m}^{-2}\cdot\text{h}^{-1}$  and  $6.29 \text{ mg}\cdot\text{m}^{-2}\cdot\text{h}^{-1}$  for control  
49 sediment. Clean soil controls internal  $\text{NH}_4^+$ -N release through cation  
50 (mainly  $\text{Al}^{3+}$ ) exchange mechanisms, while for SRP, clean soil can not only  
51 react with SRP due to its high Al and Fe content, but also stimulate the  
52 migration of active  $\text{Ca}^{2+}$  to the capping layer, thus precipitating as  
53 **Ca-bound P (Ca-P)**. Clean soil capping also contributed to the restoration  
54 of macrophytes during the growing season. However, the effect of  
55 controlling internal nutrient loading only lasted for one year under in-situ  
56 conditions, after which the sediment properties returned to pre-capping  
57 conditions. Our results highlight that clean Ca-poor soil is a promising  
58 capping material and further research is needed to extend the longevity of  
59 this geoengineering technology.

60 **Key words:**

61 Eutrophication; Internal nutrient loading; Capping; Ca-poor clean soil;  
62 Sediment-water interface; Shallow lakes

63 **1. Introduction**

64 Eutrophication of lakes arising from excessive nitrogen (N) and  
65 phosphorus (P) input leads to harmful algal blooms and retrogressive lake  
66 evolution (Bullerjahn et al., 2016). The algae compete for light with  
67 submerged vegetation, causing a shift from a macrophyte-dominated lake  
68 to algae-dominated. This leads to degradation of the physical and chemical  
69 environment beyond the point where self-recovery is possible, with the  
70 lake becoming green, turbid and foul-smelling, and potentially threatening  
71 drinking water sources (Guo, 2007; Scheffer and Nes, 2007).  
72 Geo-engineering solutions typically focus on controlling the input of  
73 external nutrients, however even once these are reduced or stopped there  
74 can be persistent release of internal N and P loads that may continue to  
75 cause eutrophication for years or even decades (Spears et al., 2014; Watson  
76 et al., 2016).

77 Research has shown that both N and P can be limiting nutrients, and  
78 hence controlling both is the most effective way to limit eutrophication  
79 (Cotner, 2017; Paerl et al., 2016). In-situ capping of lake bed sediment is  
80 considered a cost-effective technology for effectively isolating sediment  
81 nutrients and preventing or severely reducing their release (Gu et al., 2017;  
82 Lurling et al., 2016). Capping materials can include artificially  
83 chemically-modified adsorbents such as lanthanum-modified bentonite  
84 Phoslock<sup>TM</sup> (Copetti et al., 2016), iron-modified zeolite (Zhan et al., 2019),  
85 and hydrous aluminum oxide (Li et al., 2017). However, depending on the  
86 pH of the lake, these can lead to undesired chemical releases, including of  
87 toxic trivalent aluminum ions ( $Al^{3+}$ ) at pH <6, or release of lanthanum  
88 (Peterson et al., 1976; Figueiredo et al., 2022). Capping materials that  
89 cause conditions to become more alkaline can lead to the conversion of  
90  $NH_4^+$ -N into  $NH_3$ , which is toxic to biota. Balancing the available active  
91 ions in a chemically-modified capping layer with the available nutrients  
92 that need locking up (e.g. SRP) is difficult but important because excess

93 capping material capacity will lead to potential toxicity from the Al/La and  
94 NH<sub>3</sub> (Gibbs and Hickey, 2018). Iron-modified capping materials can be  
95 effective but they tend to form sediment Fe-P which is easily dissolved and  
96 released under seasonal hypoxia (Yang et al., 2020). The use of natural  
97 clean soil as a capping material can avoid these potential toxic chemical  
98 side effects, reducing both internal nutrient release and sediment  
99 resuspension with excellent ecological safety (Pan et al., 2012a; Zhong et  
100 al., 2022).

101 Evaluation of the efficiencies of capping materials for preventing  
102 nutrient release are generally conducted under laboratory conditions,  
103 and/or with short term small-scale field trials. Both approaches are limited  
104 because natural lakes are subject to seasonal and episodic hydrodynamic  
105 and temperature fluctuations, which in turn alter the sediment stability and  
106 lake biogeochemistry significantly. Longer term field testing is essential to  
107 thoroughly test the efficacy of capping approaches to control internal  
108 loading.

109 Shallow lakes are characterized by frequent hydrodynamic  
110 disturbances that lead to resuspension and deposition of bed sediments and  
111 the deposition of nutrient-rich suspended particular matter (SPM) (Xu et  
112 al., 2017). This presents a challenge for using capping layers to control  
113 internal release of nutrients because these caps themselves can be  
114 remobilized (Liu et al., 2019; Liu et al., 2016). Re-suspension events  
115 create fresh sediment-water interfaces that can be highly reactive, leading  
116 to a pulse of nutrients being released. At the same time, the material that is  
117 removed becomes SPM, mainly comprised of inorganic metal-enriched  
118 particles and organic matter, with large reactive surface area for binding  
119 any dissolved N and P. These particles, and any nutrients they have  
120 scavenged, then settle out of the water column to be re-deposited on top of  
121 the newly formed sediment-water interface, ultimately burying it again  
122 (Huser et al., 2016; Yu et al., 2017). Lakes that are subject to significant

123 input of external SPM will have the potential for this particulate material  
124 to remove nutrients from the water column into the bed sediment, where  
125 they may later become released once buried and conditions **change**.

126 The long-term effectiveness of **sediment capping under** in-situ lake  
127 environments is poorly understood (Lin et al., 2019). Hence, in this study,  
128 a three-year experimental monitoring approach was adopted, with in-situ  
129 control enclosures (uncapped) compared against enclosures where the  
130 sediment was capped with clean soil. Nutrient fluxes, porewater nutrient  
131 profiles and nutrient fraction transformations were monitored to  
132 understand nutrient dynamics and the impact of capping. The aim was to  
133 understand the impact of long term in-situ capping with clean soil on  
134 nutrient release and hence to provide a reference point for this approach to  
135 the management of waterbody eutrophication.

## 136 **2. Materials and Methods**

### 137 **2.1 Site and material description**

138 The field enclosure experiment was conducted in Shiba Bay (Fig. 1) in  
139 the northern part of Lake Taihu, China. Lake Taihu is situated on the  
140 Yanqitze delta in a highly industrialized and economically developed area  
141 of eastern China. The lake is relatively shallow (~1.5m), impacted by the  
142 southeast monsoon, and prone to annual cyanobacterial blooms, severe  
143 algal deposition, and water quality problems, which have led to the severe  
144 accumulation of internal nutrient loading (Qin et al., 2007).

145 The clean soil material used for capping was collected on the shore of  
146 Shiba Bay at Wuxi City, air dried and passed through a 40 mesh (380  $\mu\text{m}$ )  
147 screen before being applied. Table 1 shows its detailed composition,  
148 notably, clean soil has a lower Ca content than the native lake sediments.

### 149 **2.2 Field enclosure experiment design and sampling**

150 **Fig.1** shows the location of the field enclosures and the sampling sites  
151 within the enclosures. A **~70000 m<sup>2</sup> treatment and a ~50000 m<sup>2</sup> control**  
152 **enclosure were** constructed with polyvinyl chloride (PVC), aiming to

153 prevent material exchange with the external water body. In the treatment  
154 enclosure, several sub-enclosures were established, including clean sand,  
155 Ca-poor soil, chitosan modified soil capping, etc. For Ca-poor soil capping  
156 treatment, pre-processed clean soil for capping was sprayed into one  
157 enclosure water body and left to sink to the surface of the sediment,  
158 producing a capping layer of 5 cm to 10 cm thickness (Fig. S1). This  
159 capping layer depth was based on our previous experimental work to  
160 prevent resuspension (Pan et al., 2012a; Pan et al., 2019), which suggested  
161 a minimum of 1cm, and the aim to allow macrophyte growth, which  
162 requires 5-10cm for establishment and anchoring of roots. The control  
163 enclosure without capping was located adjacent to the capping enclosure.

164 Capping was undertaken in January 2010. In-situ porewater samples  
165 were collected 450d, 360d, 150d and 90d prior to capping and both  
166 porewater samples and intact sediment cores were collected 60 d and 30 d  
167 pre-capping, as well as 30d, 60d, 90d, 180d, 270d, 360d, 480d, 570d and  
168 660d post-capping. The in-situ porewater equilibration sampling devices  
169 (Peepers) were placed through the SWI by fixing to bamboo poles (Fig. S1)  
170 and left to equilibrate for 15 d before being retrieved. Intact sediment cores  
171 were sampled using a gravity core sampler (90 mm diameter, 60 cm length,  
172 Rigo Co. Ltd., Japan). All porewater samples and sediment cores were  
173 transported to the laboratory within 6 h for subsequent experiments.  
174 Incubation experiments on intact sediment cores were used to measure  
175 fluxes of  $\text{NH}_4^+\text{-N}$  and SRP at the SWI under in-situ temperature and DO  
176 conditions. Details of the sediment core incubations and in-situ peeper  
177 experiments are given in the Supplementary material. Additionally,  
178 triplicate sediment cores were also collected for the analysis of sediment  
179 oxygen demand (SOD) using dissolved oxygen microprobe technology  
180 (Presens, Regensburg, Germany). See our previous work for detailed  
181 methods (Zhong et al., 2018).

### 182 **2.3 Sediment sampling and analysis**

183 After the sediment incubation experiments, the top 0-2 cm of the  
184 sediment cores were sliced for surface sediment properties analysis. Fresh  
185 sediment subsamples were used to analyze the total microbial activity of  
186 sediments according to the method described by [Schnürer and Rosswall](#)  
187 [\(1982\)](#). Then, three surface sediment samples were pooled and  
188 homogenized to obtain a representative sample for further analysis. The  
189 fresh surface sediment was lyophilized under a vacuum, and ground, then  
190 passed through 0.150 mm sieves, and stored at 4 °C until subsequent  
191 analysis.

192 The total nitrogen (TN) content of surface sediment was analyzed by  
193 the alkaline potassium persulfate oxidation method ([Chinese EPA, 2002](#)).  
194 Sediment dissolved inorganic nitrogen (DIN), including  $\text{NH}_4^+\text{-N}$ ,  $\text{NO}_3^-\text{-N}$   
195 and  $\text{NO}_2^-\text{-N}$  was extracted by 2 mol/L KCl and analyzed by UV  
196 spectrophotometer ([Shannon et al., 2011](#)). Acid microwave digestion was  
197 used to determine Al, Fe, Ca, Mn, Ni, Zn, Cu and Cr by ICP-AES ([Rukun,](#)  
198 [1999](#)). Sediment organic matter content was measured as loss of ignition  
199 (LOI) and determined by calcination at 550 °C for 6h. Sediment  
200 phosphorus (P) fractions were extracted based on the method reported by  
201 [Rydin \(2000\)](#) and were grouped as labile P ( $\text{NH}_4\text{Cl-P}$ ), redox-sensitive P  
202 ( $\text{Fe-P}$ ), aluminum-bound P ( $\text{Al-P}$ ), organic P ( $\text{Org-P}$ ), other inorganic P  
203 ( $\text{Ca-P}$ ) and residual P ( $\text{Res-P}$ ). Sediment total P was calculated as the sum  
204 of above fractions. Further details of the extraction process are given in  
205 [Fig. S2](#) in the supplementary materials.

#### 206 **2.4 Phosphate adsorption isotherm experiments**

207 Phosphate adsorption isotherms were determined using the method  
208 and calculation procedures in [Pan et al. \(2002; 2013\)](#) and [Yu et al. \(2017\)](#).  
209 Briefly, 0.5g of the processed surface sediment was added to 40ml of the  
210 solution, and mixed in 50ml polyethylene tube. The P concentration  
211 gradient of the solutions was set to 0, 0.05, 0.2, 0.5, 1, 2, 5 and 10mg/L.  
212 The mixture was incubated for 48h in a constant temperature shaker at 180



213 rpm and 25 °C. After the incubation, the supernatant was obtained by  
214 centrifugation at 5000 rpm and filtered through a GF/C membrane for  
215 analysis. Finally, the maximal adsorption capacity ( $Q_{\max}$ , mg/g) and zero  
216 equilibrium P concentration ( $EPC_0$ , mg/L) were calculated by the  
217 non-linear form of the Langmuir equation to characterize the P adsorption  
218 capacity of surface sediments.

## 219 **2.5 Statistical analysis**

220 One-way analysis of variance (ANOVA) with Tukey's post hoc test  
221 was used to identify the significant differences in nutrient fluxes,  
222 porewater nutrient concentrations, and sediment properties between control  
223 and capping treatment. Pearson's correlation analysis was used to examine  
224 the relationships between nutrient fluxes and environmental variables.  
225 Significant difference was set at the  $p < 0.05$  level. Statistical analysis was  
226 performed using SPSS 25.0 (IBM, New York, USA).

## 227 **3. Results**

### 228 **3.1 Characteristics of clean soil and surface sediment**

229 The physicochemical characteristics of the clean soil and surface  
230 sediment are shown in Table. 1 and Fig. 2. The results show that the clean  
231 soil is characterized by lower organic matter (LOI), TP and TN and Ca  
232 content with slightly higher Al and Fe content than the surface sediment  
233 (Table. 1, Fig. 2). This plays a role in systematic differences measured  
234 between the capping sediment and uncapped control sediment 30 days  
235 post-capping, where the average values of the former are 95% LOI, 46%  
236 TP, 52% TN, 31% (Ca), 110% (Al) and 130% (Fe) of those of the latter.  
237 Furthermore, lower Mn, Ni, Zn, Cu and Zr contents were measured in the  
238 clean soil, indicating its suitability as an ecologically safe capping material.  
239 **When** the Ca-poor soil was introduced into the waterbody, the contents of  
240 TP and Ca in the capping sediment **increased** rapidly within 60d after  
241 capping, from 344 mg·kg<sup>-1</sup> and 2.02 mg·g<sup>-1</sup> to 644 mg·kg<sup>-1</sup> and 5.13 mg·g<sup>-1</sup>,  
242 respectively (Table. 1).

243 The sediment oxygen demand (SOD) of both capping and control  
244 treatment showed significant seasonal variability within one year of  
245 capping (Fig. S3). The highest SOD rates appeared in summer (180d) and  
246 capping and control treatment only showed significant differences in  
247 summer. The total microbial activity of the control sediment showed  
248 significant seasonal variation (Fig. S4), and was highest in summer (180d),  
249 while the capping sediments did not show significant seasonal variation.  
250 Consequently, a significant difference between microbial activity in the  
251 capping and control treatments was only found in summer.

### 252 3.2 Fraction of N and P in capping and control sediments

253 The variation of DIN of the surface sediment in control and capping  
254 sediments is shown in Fig. 2. Sediment  $\text{NH}_4^+\text{-N}$  content decreased  
255 significantly after capping, reaching 57% of control sediment values 30d  
256 post-capping, and then increased before further fluctuation. Sediment TN  
257 also decreased post capping but then increased to levels similar to the  
258 control. No significant difference was observed in  $\text{NO}_3^-\text{-N}$  and  $\text{NO}_2^-\text{-N}$   
259 between control and capping sediment.

260 The variation of different P fractions in control and capping sediments  
261 were displayed in Fig. 3 and Fig. S5. The dominant surface sediment P  
262 fractions were Fe-P, Al-P and Ca-P prior to capping, averaging 27.20%,  
263 24.55% and 22.49% respectively. The capped sediments then evolved such  
264 that Al-P, Fe-P and Res-P became the dominant fractions (averaging  
265 31.44%, 21.79% and 15.70% respectively). Furthermore, beyond 30d after  
266 capping, the inert P (the sum of Al-P, Ca-P and Res-P) in the capping  
267 sediment increased significantly compared with the control sediment,  
268 averaging 62.60% of TP (Fig. S5). Sediment Ca-P content increased from  
269 2.00 mg/kg at 30d post-capping to 104.29 mg/kg at 660d post-capping, a  
270 50-fold increase respectively (Fig. 3).

271 Positive correlations ( $p < 0.05$ ) were found between sediment Ca-P,  
272 TP and Ca content, between Fe, Al and Res-P, and also between Al-P and

273  $\text{NH}_4^+\text{-N}$ , and  $\text{NH}_4^+\text{-N}$  and TN (Fig. S6). Significant negative correlations ( $p$   
274  $< 0.05$ ) were found between Res-P, Fe and Ca-P content and between Fe,  
275 Al and  $\text{NO}_3^-\text{-N}$  content, except for between Res-P and Fe, and Fe and Al  
276 content in the sediment.

### 277 3.3 Phosphate adsorption capacity of capping and control sediments

278 A Langmuir model was used to fit the equilibrium adsorption data of  
279 SRP on the surface sediment and clean capping soil (Pan et al., 2002),  
280 results are shown in Fig. 4 and detailed parameters are listed in Table. S1.  
281  $\text{EPC}_0$  of the capping sediments was significantly lower than that of the  
282 control sediment. Furthermore, the  $Q_{\max}$  values for the control and capping  
283 sediment were 0.2 mg/g to 0.31 mg/g and 0.24 mg/g to 0.35 mg/g,  
284 respectively, and the clean soil was 0.36 mg/g.  $K_p$  values for retention  
285 capacity of solid phase for SRP were 0.03 L/g to 0.54 L/g and 0.43 L/g to  
286 4.27 L/g for the control and capping sediment respectively, and the clean  
287 soil was 6.75 L/g. All the above parameters show that the capping sediment  
288 was characterized by greater P adsorption and retention capacity than the  
289 control sediment, except at the end of the 660-day experiment.

### 290 3.4 Nutrients porewater concentrations and fluxes across the SWI

291 The temporal variation of control and capping sediment porewater  
292 nutrient concentrations with sediment depth are shown in Fig. 5. and Fig. 6.  
293 For  $\text{NH}_4^+\text{-N}$ , the pre-capping sediments show a good degree of  
294 homogeneity, with similar profiles of low overlying water concentrations  
295 and then increasing concentrations with depth below the SWI reaching a  
296 stable value at about -10cm, with steeper gradients during the warmer  
297 sampling periods. Post-capping  $\text{NH}_4^+\text{-N}$  profiles remain largely unchanged  
298 in both control and capped systems, which show no significant differences.  
299 For SRP, the pre-capping profiles show similar sharp increases in  
300 concentration immediately below the SWI and generally peaked at about  
301 -2cm to -5cm, with variations reflecting temperatures of sampling periods.  
302 Post-capping profiles show clear differences between the control sites and

303 the capped sites. Capping caused burial of previous SRP peaks and then a  
304 homogenization of profiles at lower levels of SRP which took a long period  
305 (> 1 year) to re-establish diffusive gradients.

306 **Fig. 7.** shows  $\text{NH}_4^+\text{-N}$  fluxes across the SWI in the control sediment  
307 varied from  $3.08 \pm 1.03 \text{ mg}\cdot\text{m}^{-2}\cdot\text{h}^{-1}$  to  $300.68 \pm 53.95 \text{ mg}\cdot\text{m}^{-2}\cdot\text{h}^{-1}$ , peaking  
308 at 180d post-capping in summer. Capped sediments exhibited similar  
309 temporal patterns, varying from  $4.16 \pm 1.31 \text{ mg}\cdot\text{m}^{-2}\cdot\text{h}^{-1}$  to  $107.57 \pm 40$   
310  $\text{mg}\cdot\text{m}^{-2}\cdot\text{h}^{-1}$ , with a peak at 180d, and second smaller peak ( $23.82 \pm 12.11$   
311  $\text{mg}\cdot\text{m}^{-2}\cdot\text{h}^{-1}$ ) at 570d in summer. All measurements showed  $\text{NH}_4^+\text{-N}$  efflux  
312 from the sediment to the overlying water. Capping significantly ( $p < 0.05$ )  
313 reduced  $\text{NH}_4^+\text{-N}$  efflux for one year compared to control sediments, but  
314 this effect disappeared thereafter.

315 SRP fluxes of control sediment (**Fig. 7**) show similar temporal trends  
316 to  $\text{NH}_4^+\text{-N}$  fluxes, varying from  $0.24 \pm 0.04 \text{ mg}\cdot\text{m}^{-2}\cdot\text{h}^{-1}$  to  $26.97 \pm 1.91$   
317  $\text{mg}\cdot\text{m}^{-2}\cdot\text{h}^{-1}$ , with a first peak at 180d post-capping and second smaller peak  
318 ( $9.93 \pm 4.10 \text{ mg}\cdot\text{m}^{-2}\cdot\text{h}^{-1}$ ) at 570d post-capping in summer. SRP fluxes in the  
319 capped sediment switched from effluxes to influxes from 90d, reaching a  
320 maximum influx of  $-4.94 \pm 2.17 \text{ mg}\cdot\text{m}^{-2}\cdot\text{h}^{-1}$  at 180d post-capping, before  
321 then switching back to effluxes, with a peak of  $9.05 \pm 2.94 \text{ mg}\cdot\text{m}^{-2}\cdot\text{h}^{-1}$  at  
322 570d. Fluxes were therefore significantly ( $p < 0.05$ ) different to controls  
323 for the first year, but this difference disappeared during the second year.  
324 Notably, a significant ( $p < 0.05$ ) positive correlation was obtained between  
325 SRP flux and sediment Fe-P content (**Fig. S6**).

## 326 **4. Discussion**

### 327 **4.1 Clean soil capping controls $\text{NH}_4^+\text{-N}$ and SRP fluxes at the SWI**

328 In this study, **Fig. 7** shows that clean soil capping produces an average  
329 of 31% reduction of internal  $\text{NH}_4^+\text{-N}$  fluxes from the sediment for one year.  
330 Simultaneously, capping caused SRP fluxes to switch from efflux to influx  
331 for one year after capping, with the source-sink transition between  
332 overlying water and sediment. Overall, clean soil capping effectively

333 controlled internal  $\text{NH}_4^+$ -N and SRP release for up to one year, but not  
334 thereafter.

335 The diffusion of N and P from sediment to overlying water mainly  
336 depends on the concentration gradient at the SWI. Higher  $\text{NH}_4^+$ -N fluxes  
337 across the SWI consistent with higher porewater  $\text{NH}_4^+$ -N concentrations  
338 were measured in warm seasons (Fig. 7), where the elevated temperature  
339 enhanced rates of microbial activity (Fig.S4), increasing the mineralization  
340 of organic matter, depleting dissolved oxygen and enhancing anaerobic  
341 conditions with sediment depth (Fig. S3) (Ding et al., 2018). A  
342 combination of enhanced degradation of organic matter and reduced  
343 nitrification caused increased accumulation of  $\text{NH}_4^+$ -N, leading to steeper  
344 pore-water gradients and enhanced efflux (Beutel, 2006; Zhong et al.,  
345 2021). Reduced  $\text{NH}_4^+$ -N effluxes in the capping sediment compared to the  
346 control were likely due to the clean soil providing additional cation  
347 exchange capacity that led to sorption of  $\text{NH}_4^+$ -N when diffusing across the  
348 capping layer. This ultimately reduced the  $\text{NH}_4^+$ -N concentration of the  
349 overlying water (Leyva-Ramos et al., 2008; Pan et al., 2012b; Zhan et al.,  
350 2019).

351 In parallel, clean soil capping resulted in a reduction in porewater  
352 SRP concentration and a switch from SRP effluxes to influxes. This result  
353 is attributed to the immobilization of SRP by the clean soil. Prior to  
354 capping, SRP was being liberated at depth due to anaerobic conditions,  
355 most likely through a combination of release from degrading organic  
356 matter and release from iron oxyhydroxides during microbial iron  
357 reduction (Tammeorg et al., 2020). Addition of clean soil caused a  
358 reduction in SRP generation at depth and led to the sediment becoming a  
359 sink for P, thus the SRP concentration of the overlying water was  
360 effectively reduced (Pan et al., 2012b, Pan et al., 2019). This is most likely  
361 due to oxygenated soil containing abundant iron oxides and other reactive  
362 surface sites causing simultaneous retardation of anerobic microbial

363 activity and sorption of SRP (Hinsinger, 2001; Moore et al., 1994). The  
364 increased SRP influx during warmer sampling periods is likely due to  
365 enhanced microbial degradation during those periods producing more SRP  
366 available to be locked up by the sediment iron oxides (Figs 7, S3), and the  
367 lack of accumulation of SRP in the pore-water suggests there are sufficient  
368 iron oxides in the sediment to immediately adsorb any SRP produced. This  
369 is further supported by the good SRP sorption and retention capacity of the  
370 clean soil (Fig. 4; Table. S1). The above processes explain why SRP fluxes  
371 were significantly positively correlated with sediment Fe-P content, with  
372 smaller SRP influx at higher Fe-P content. Moreover, porewater SRP  
373 concentrations of capping sediment within -10 cm reduced to range from  
374 0.0005 mg·L<sup>-1</sup> to 0.40 mg·L<sup>-1</sup> compared to 0.04 mg·L<sup>-1</sup> to 1.84 mg·L<sup>-1</sup> in  
375 control sediment, indicating the presence of a static layer directly below  
376 the SWI after the clean soil capping, which has been confirmed to play a  
377 key role in controlling internal P desorption and mobilization from the  
378 sediment to overlying water across the SWI (Wang et al., 2017).

379 Temporally, the internal NH<sub>4</sub><sup>+</sup>-N and SRP fluxes recovered after one  
380 year of capping. Our results suggest a continuous process of transformation  
381 from clean soil to native sediment, leading to the return of  
382 physicochemical properties towards those of the initial sediment (Table 1).  
383 Recovered NH<sub>4</sub><sup>+</sup>-N fluxes may attributed to NH<sub>4</sub><sup>+</sup>-N being able to transfer  
384 across the capping layer unhindered, as any cation capacity to absorb it  
385 was used up. Meanwhile, a switch of SRP influxes to effluxes was detected,  
386 corresponding with steeper SRP concentration gradient at the SWI (Fig. 6),  
387 which supported the internal SRP release (Wen et al., 2020). This was  
388 further supported by a weakening of the SRP sorption and retention  
389 capacity effect of the clean soil (Fig. 4).

#### 390 **4.2 Underlying mechanisms of clean soil capping to control porewater** 391 **NH<sub>4</sub><sup>+</sup>-N and SRP concentrations**

392 Our results show that clean soil can effectively control porewater SRP

393 concentration but not  $\text{NH}_4^+$ -N concentrations (Fig. 5 and Fig. 6). Porewater  
394  $\text{NH}_4^+$ -N concentration is significantly negatively correlated with the  
395 sediment Al ion content (Fig. S6), thus we deduced that cation exchange  
396 between the exchangeable cations in the clean soil (Al ion) and  $\text{NH}_4^+$ -N in  
397 porewater is an important mechanism for the adsorptive removal of  
398  $\text{NH}_4^+$ -N from the porewater and controls its released from the clean soil  
399 sediment caps (Alshameri et al., 2014; Lin et al., 2013; Lin et al., 2014).  
400 This is supported by the fact that the clean soil has a higher Al and Fe  
401 content than the sediment, and that this reduces with time (Table 1).  
402 Finally, sediment  $\text{NH}_4^+$ -N shares the same temporal variation with  
403 sediment TN, and is also positively correlated with sediment Al-P content  
404 (Fig. S6). This supports the hypothesis that  $\text{NH}_4^+$ -N is adsorbed by the  
405 clean soil. This process could release  $\text{Al}^{3+}$ , then promoting the reaction of  
406  $\text{Al}^{3+}$  and SRP in porewater to form Al-P (Fig. 8). Moreover, the aerobic  
407 environment caused by clean soil capping could promote sediment  
408 microbial activity, particularly nitrifying bacteria, thus  $\text{NH}_4^+$ -N is  
409 decreased in short term (Pan et al., 2019; Zhang et al., 2021). However, the  
410 presence of a large amount of organic N in the sediment (Fig. 2) can  
411 quickly replenish the porewater  $\text{NH}_4^+$ -N concentration, which explains why  
412 the clean soil capping has limited impact on porewater  $\text{NH}_4^+$ -N  
413 concentrations but can significantly reduce the  $\text{NH}_4^+$ -N fluxes at the SWI.  
414 Vertically, the  $\text{NH}_4^+$ -N concentration in porewater increased with depth in  
415 the sediment and reached a maximum stable value at -10 cm, which is  
416 consistent with our previous study (Zhong et al., 2018). The highly  
417 anaerobic conditions at depth are conducive to the accumulation of  $\text{NH}_4^+$ -N  
418 (Roberts et al., 2012), while nitrification is inhibited and denitrification  
419 was promoted, thus promoting the desorption of  $\text{NO}_2^-$ -N, an intermediate  
420 product of denitrification, from the sediment, explaining the negative  
421 correlation of sediment  $\text{NO}_2^-$ -N and porewater  $\text{NH}_4^+$ -N (Zhong et al., 2010a;  
422 Zhong et al., 2010b). The possible explanation for the negative correlation

423 with sediment Res-P content was that capping leads to an increase in pH  
424 which promotes the desorption and release of Res-P (Zhou et al., 2019).

425 Fig. 6 shows that clean soil capping is effective at controlling  
426 porewater SRP. This can be attributed to the higher Fe content of the clean  
427 soil (Table. 1). Previous studies have confirmed that the ligand exchange  
428 of Fe oxide/hydroxide with SRP to form an inner-sphere P-O-Fe link plays  
429 an important role in SRP uptake (Ajmal et al., 2018; Cao et al., 2016).  
430 Furthermore, since SRP and  $\text{NH}_4^+\text{-N}$  coexist in the porewater, it is possible  
431 that the  $\text{Al}^{3+}$  can be desorbed from the clean soil via cation exchange  
432 between  $\text{Al}^{3+}$  on the clean soil and porewater  $\text{NH}_4^+\text{-N}$ , allowing it to then  
433 react with SRP to form Al-P (Fig. 8). Therefore, clean soil capping has a  
434 better SRP adsorption capacity to control internal P release due in part to a  
435 combination of the high Fe and Al present. This can be further supported  
436 by the significant positive correlation between the sediment Fe and Al  
437 content and sediment Res-P (Fig. S6), indicating that the presence of Fe  
438 and Al can promote the formation of inert P which is consistent with the  
439 result that lower SRP concentration was observed in the porewater (Zhan et  
440 al., 2019). Notably, sediment Ca content increased from 1.99 mg/g to 5.32  
441 mg/g over the whole experiment (Table. 1), and the migration of Ca could  
442 accelerate the chemical precipitation of porewater SRP with  $\text{Ca}^{2+}$  to form  
443 Ca-P, thereby transforming the porewater SRP to sediment inert P (Lin et  
444 al., 2011). Therefore, we conclude that the control mechanism of porewater  
445 SRP by clean soil capping was likely a combination of SRP adsorption due  
446 to the higher Fe and Al content, and the co-precipitation of  $\text{Ca}^{2+}$  with  
447 porewater SRP (Fig. 8). Clean soil capping can effectively reduce SRP  
448 concentrations in porewater within one year, which was also confirmed by  
449 our previous short-term work (Pan et al., 2019). However, the porewater  
450 SRP concentrations recovered gradually after one-year post-capping due to  
451 a combination of increased sediment P loading and the weakened P  
452 adsorption and retention capacity (Fig. 4) (Wen et al., 2020).



### 453 **4.3 Variation of P fractions in surface sediments after capping**

454 Sediment P release potential is determined by various P fractions in  
455 sediment and their relative abundance (Liu et al., 2022; Rydin, 2000). The  
456 upper 2cm of the control and capping sediment contained different P  
457 fractions (Fig. 3).

458 Sediment total P (TP) is the sum of different P fractions. Fig. 3 shows  
459 that the TP of capping sediment increased significantly and approached  
460 that in the control sediment within the first year after capping, while the  
461 TP content of control sediment maintained high values throughout. This is  
462 associated with the isotherm parameters determined by the Langmuir  
463 equation, the  $Q_{\max}$  and  $K_p$  decrease from  $0.36 \text{ mg}\cdot\text{g}^{-1}$  to  $0.32 \text{ mg}\cdot\text{g}^{-1}$  and  
464  $6.75 \text{ L}\cdot\text{g}^{-1}$  to  $0.43 \text{ L}\cdot\text{g}^{-1}$  within one-year (Table. S1), suggesting the  
465 reduced P adsorption and retention capacity of capping sediment, mainly  
466 due to the reducing difference in the TP content compared to the control  
467 sediment (Lai and Lam, 2009; Wen et al., 2020). The variations of different  
468 P fractions in the capping sediment were significant. Previous studies have  
469 confirmed that mobile P (the sum of  $\text{NH}_4\text{Cl-P}$ ,  $\text{Fe-P}$  and  $\text{Org-P}$ ) is  
470 considered algal-available and hence a potential internal P loading while  
471 inert P (the sum of  $\text{Al-P}$ ,  $\text{Ca-P}$  and  $\text{Res-P}$ ) is considered a pool of  
472 permanent burial P which is hard to release (Rydin, 2000). Our results  
473 showed that clean soil capping can significantly reduce the mobile P  
474 content in the surface sediments (Fig. 3 and Fig. S5).  $\text{NH}_4\text{Cl-P}$  corresponds  
475 to immediately algal-available P, which is adsorbed to the surface of  
476 sediment particles (Sun et al., 2009). An apparent reduction of  $\text{NH}_4\text{Cl-P}$  in  
477 capping sediment was observed, reducing from  $3.97 \text{ mg}\cdot\text{kg}^{-1}$  to  $1.43$   
478  $\text{mg}\cdot\text{kg}^{-1}$  compared to the control (Fig. 3), suggesting that clean soil capping  
479 can effectively control labile P. This apparent decrease is attributed to the  
480 introduction of clean soil characterized by excellent P adsorption capacity  
481 that removes labile P by physical adsorption to soil particulates (Zhou et  
482 al., 2019). This phenomenon is further supported by reduced porewater

483 SRP concentration within the clean soil capping layer.

484 Fe-P is redox-sensitive P, which easily released under anaerobic  
485 conditions and transformed to potential algal-available P (Chen et al.,  
486 2015). Fig. 3 and Fig. S5 show a decrease of mobile P in the capping  
487 sediment mainly originated from Fe-P, accounting for 128.7% of decreased  
488 mobile P and 92% of TP. The clean soil characterized by a high Fe that  
489 promotes the reaction of  $\text{Fe}^{3+}$  with SRP to form Fe-P under aerobic  
490 conditions during the cold season. And the lack of Ca-P together then  
491 results in the increased ratio of mobile P to TP in the early period after  
492 capping. Microbial activity and SOD were promoted by increased  
493 temperatures (Figs. S3, S4), leading to anaerobic conditions within the  
494 sediment during warm seasons, with Fe-P readily released due to the  
495 reduction of  $\text{Fe}^{3+}$  to  $\text{Fe}^{2+}$  (Wang et al., 2016). Org-P increased slightly  
496 early in the experiment but decreased during the warm season accompanied  
497 by dissolution of Fe-P in the uncapped sediment, however, the opposite  
498 variation was observed in capping sediment. This indicates different P  
499 release mechanisms between control and capping sediment, the control  
500 sediment being mainly controlled by coupled release of Fe-P and Org-P  
501 while the capping sediment is dominated by the traditional Fe-P release  
502 process, demonstrating the shift of internal P release processes after  
503 capping (Liu et al., 2022; Sun et al., 2022). Notably, there is a negative  
504 correlation between sediment Fe and Ca-P content, which gives the likely  
505 explanation of competitive adsorption on P by stronger reactive  $\text{Ca}^{2+}$  and  
506  $\text{Fe}^{3+}$ , promoting the shift of Fe-P to Ca-P, a similar phenomenon to that  
507 reported by Zhou et al. (2019).

508 Our results show that inert P increased sharply within one year of  
509 capping (Fig. 3), which is mainly attributed to the increase of Ca-P and  
510 Al-P. This result indicated that capping is beneficial for the formation of  
511 inert P fractions in the sediment (Li et al., 2019; Yin et al., 2021), which is  
512 further supported by the lower porewater SRP concentration observed in

513 the capping sediment (Fig. 6). Al-P is often analyzed together with Fe-P,  
514 and while Al-P is actually more difficult to re-release than Fe-P, our result  
515 found that sediment Al-P was positively correlated with sediment  $\text{NH}_4^+\text{-N}$ ,  
516 implying that the released  $\text{Al}^{3+}$  is from cation exchange between sediment  
517  $\text{Al}^{3+}$  and  $\text{NH}_4^+\text{-N}$  in porewater, thus promoting the formation of Al-P  
518 (Rönicke et al., 2021; Rydin, 2000). Furthermore, the Al-P content reduced  
519 while the Ca-P content increased after 60d post-capping, which may be  
520 attributed to the actively competitive adsorption of P by  $\text{Ca}^{2+}$  over  $\text{Al}^{3+}$   
521 (Yin et al., 2021). Ca-P is regarded as permanently buried P, and a  
522 significant positive correlation was found between sediment Ca-P and Ca  
523 content, consistent with our result that Ca-P accounts for 64.07% of the  
524 increased TP during the experiment. In this study, Ca-poor soil exhibited a  
525 similar excellent internal P control ability to Ca-modified material (Zhou  
526 et al., 2019). The underlying mechanism is likely the formation of a  $\text{Ca}^{2+}$   
527 concentration gradient between the Ca-poor capping layer and native  
528 surface sediment, which promotes the migration of active  $\text{Ca}^{2+}$  to the  
529 capping layer and, thus, reacts with SRP to form a precipitate of Ca-P  
530 compounds (Fig. 8). The above-mentioned shift in the release mechanism  
531 of coupled Fe-P and Org-P to Fe-P suggests the transformation of  
532 algae-dominated status to macrophyte-dominated status (Liu et al., 2022),  
533 thus the precipitation of Ca and SRP by calcite crusts on the surface of  
534 submerged macrophytes might play an important role in increased sediment  
535 Ca-P (Blindow, 1992; Sand-Jensen et al., 2021). Furthermore, the reduced  
536 sediment Res-P suggests the enhanced alkaline environment, which would  
537 allow  $\text{Ca}^{2+}$  to become the primary SRP-binding reactant over Fe and Al,  
538 and also explains the negative correlation of sediment Ca-P and Res-P  
539 content (Wu et al., 2022).

#### 540 **4.4 Implication for the development of Ca-poor capping material and** 541 **practical capping geoengineering**

542 In this study, the large-scale field experiment is close to a practical

543 geoengineering project, and hence understanding the long-term  
544 performance is important for decision-making in eutrophication  
545 management. The experimental results indicate that clean soil capping  
546 could effectively mitigate internal N and P release from sediment  
547 simultaneously for one year (Fig.7). Furthermore, clean soil is a natural  
548 ecologically-safe material that helps to change the algae-dominated status  
549 of a lake to macrophyte-dominated status (Pan et al., 2012a). In this study,  
550 the recovery of submerged macrophytes was observed during the growing  
551 season. Our results indicate that Ca-poor soil can be used in  
552 geoengineering to control internal nutrient loading and provide a better  
553 habitat for macrophytes. The dominant macrophytes observed were  
554 naturally occurring *P. malaianus* and *P. crispus*, and their recovery was  
555 accompanied by reduced Chl- $\alpha$  concentrations (Fig. S7) (Pan et al., 2012b).  
556 Previous studies on capping materials have focused on calcium-rich  
557 material, such as heat-modified Ca-rich attapulgite (Gan et al., 2009),  
558 natural/modified zeolite (Zhan et al., 2019), illite (Gu et al., 2019) and  
559 confirmed these have better capacity to control sediment internal P loading  
560 and promote the transformation of mobile P to inert P (Hinsinger, 2001).  
561 Therefore, use of clean soil characterized by lower Ca content was contrary  
562 to the widely accepted view. Interestingly, we found that when Ca-poor  
563 soil is introduced into the water body, the Ca-rich water body will  
564 automatically supplement the Ca content to the capping layer, thus  
565 achieving a similar effect to that of Ca-rich materials. This finding leads us  
566 to consider the development of Ca-poor and environment-friendly  
567 materials for geoengineering.

568 The time-limited effectiveness of geoengineering in controlling  
569 internal nutrient loading continues to plague the successful application of  
570 projects. We found that N and P fluxes accompanied with surface sediment  
571 physicochemical properties recovered one-year post-capping (Fig. 7; Table  
572 1). When the clean soil was introduced into the water body, the clean soil

573 gradually transformed to native sediment under the in-situ lake conditions.  
574 For example, the Ca-rich water body will continually supply Ca to the  
575 Ca-poor soil, thus causing changes in the P forms and Ca-P shifting  
576 process (Fig. 3). In addition, considering the background of persistent  
577 external inputs, the external input SPM has high nutrient and organic  
578 matter content could continuously deposit upon the capping layer,  
579 promoting the return of the physicochemical properties of new born SWI to  
580 the pre-capping status (Wen et al., 2020). Furthermore, surface sediment is  
581 prone to resuspension under hydrodynamic disturbance, which promotes  
582 the potential for deposition of contaminated sediment from uncapped areas  
583 to those with capping. Moreover, bioturbation will not only reorganize the  
584 sediment vertically to allow the capping material to react with deep  
585 sediment (Xu et al., 2017; Yin et al., 2021), but also can accelerate the  
586 mixing of the deposited SPM and capping material, promoting the  
587 sedimentation process of the capping material. Overall, we found that the  
588 change in the color of surface sediment (clean soil) was slow as it  
589 transformed from Ca-poor soil to native sediment after capping (Fig. S8).  
590 However, the change in the contents of Ca and Ca-P in the surface  
591 sediments (clean soil) was rapid (Table 1; Fig. 3). This result suggested  
592 that the active migration of substances (such as Ca and P) in the water body  
593 rather than sediment disturbance processes and external SPM input  
594 dominated the recovery of sediment properties and internal loading.

595 Clean soil as a natural material can effectively control internal  
596 loading of nutrients for only one year and promote macrophyte restoration  
597 for a longer period. The results of our long-term enclosure experiment  
598 cause us to worry about the long-term effects of other functional  
599 geoengineering materials. Future research should focus on the long-term  
600 effects of functional materials under field condition and how to use  
601 management measures to extend the long-term effects of geoengineering  
602 technology.

603 **5. Conclusion**

604 A three-year field enclosure experiment was carried out to investigate  
605 the long-term performance and underlying mechanism of clean soil capping  
606 on internal nutrient loading mitigation. Clean soil capping can not only  
607 reduce internal N and P fluxes and porewater SRP concentration for one  
608 year but also promote the restoration of macrophytes in a eutrophic lake.  
609 Clean soil characterized with high Al and Fe content can prevent internal  
610  $\text{NH}_4^+$ -N release through cation exchange, and also has excellent P  
611 adsorption and retention capacity. Furthermore, Ca-poor clean soil has  
612 performed better in the control of internal P release via not only high  
613 cation capacity to react with SRP in the short-term, but also via stimulating  
614 the migration of active  $\text{Ca}^{2+}$  to precipitate with SRP, thus promoting the  
615 burial of internal P in long-term. However, under the in-situ conditions of  
616 Lake Taihu, the properties of capping sediment will gradually recover to  
617 the state of the native sediment, ultimately resulting in weakened  
618 effectiveness after one-year post-capping. Our field enclosure experiment  
619 demonstrated that the clean Ca-poor soil is a promising capping material to  
620 control the internal nutrient loading and help the recovery of macrophytes,  
621 and future research efforts should be exerted to extend the longevity of this  
622 geoengineering technology.

623 **Acknowledgements**

624 The study was supported by Chinese National Basic Research Program  
625 (2008CB418105), Chinese National Key Research and Development Program  
626 (2022YFC3202703, 2022YFC3202705), and the National Natural Science Foundation  
627 of China (Grant No. 41771516). We thank Guofeng Liu, Qiushi Shen, Jingge Shang,  
628 and Mengyao Tang for their help in field sampling and experimental analysis. We also  
629 thank the editor and anonymous reviewers for their constructive comments and  
630 suggestions to help us improve the manuscript.

631

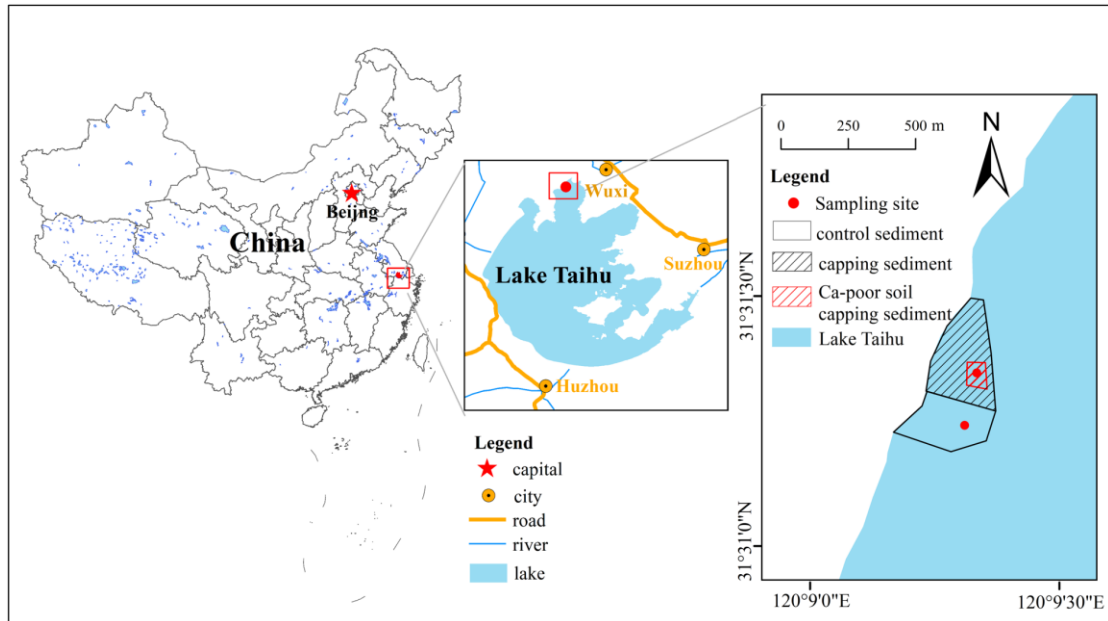
632

633  
 634  
 635  
 636  
 637  
 638  
 639  
 640  
 641  
 642  
 643  
 644  
 645  
 646  
 647  
 648  
 649  
 650  
 651  
 652

653 **Table 1.** The physical and chemical properties of clean soil, control and capping  
 654 sediment treatment during three-year experiment.

Sample	Time	LOI (%)	TP (mg/kg)	Al (mg/g)	Fe (mg/g)	Ca (mg/g)	Mn (mg/kg)	Ni (mg/kg)	Zn (mg/kg)	Cu (mg/kg)	Cr (mg/kg)
Clean soil		3.5	319	61.1	35.6	1.99	557	31	71	13	58
Control	60d pre-capping	3.7	779	55.1	27.3	6.98	902	75	259	98	111
Control	30d pre-capping	3.7	753	54.6	26.6	6.76	875	75	252	96	106
Control	30d post-capping	3.8	748	54.8	27.2	6.56	915	75	255	97	106
Control	60d post-capping	3.9	786	58.5	29.3	6.83	1006	79	264	97	119
Control	90d post-capping	4.2	781	60.1	30.1	7.17	974	79	268	103	122
Control	270d post-capping	4.2	703	53.6	26.7	6.40	835	54	195	83	115
Control	660d post-capping	4.2	647	53.9	26.7	6.78	815	64	220	84	99
Capping	60d pre-capping	4.6	816	59.3	29.1	6.38	938	78	260	101	118
Capping	30d pre-capping	4.6	855	59.8	29.7	6.55	959	78	266	101	122
Capping	30d post-capping	3.6	344	60.3	35.3	2.02	883	33	74	18	60
Capping	60d post-capping	4.0	644	58.7	31.5	5.13	873	60	200	70	99
Capping	90d post-capping	4.3	623	57.6	29.9	4.80	771	61	195	69	94
Capping	270d post-capping	4.5	609	52.5	25.0	5.21	737	61	197	70	90
Capping	660d post-capping	4.7	638	53.4	25.8	5.32	666	57	198	75	91

655  
 656



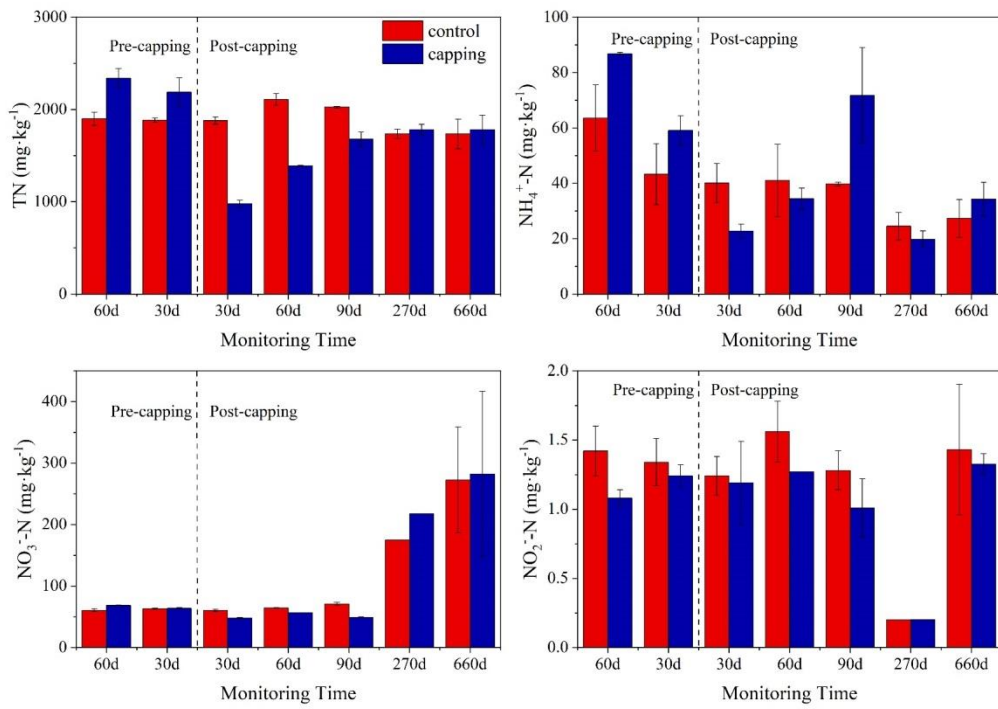
657

658

659

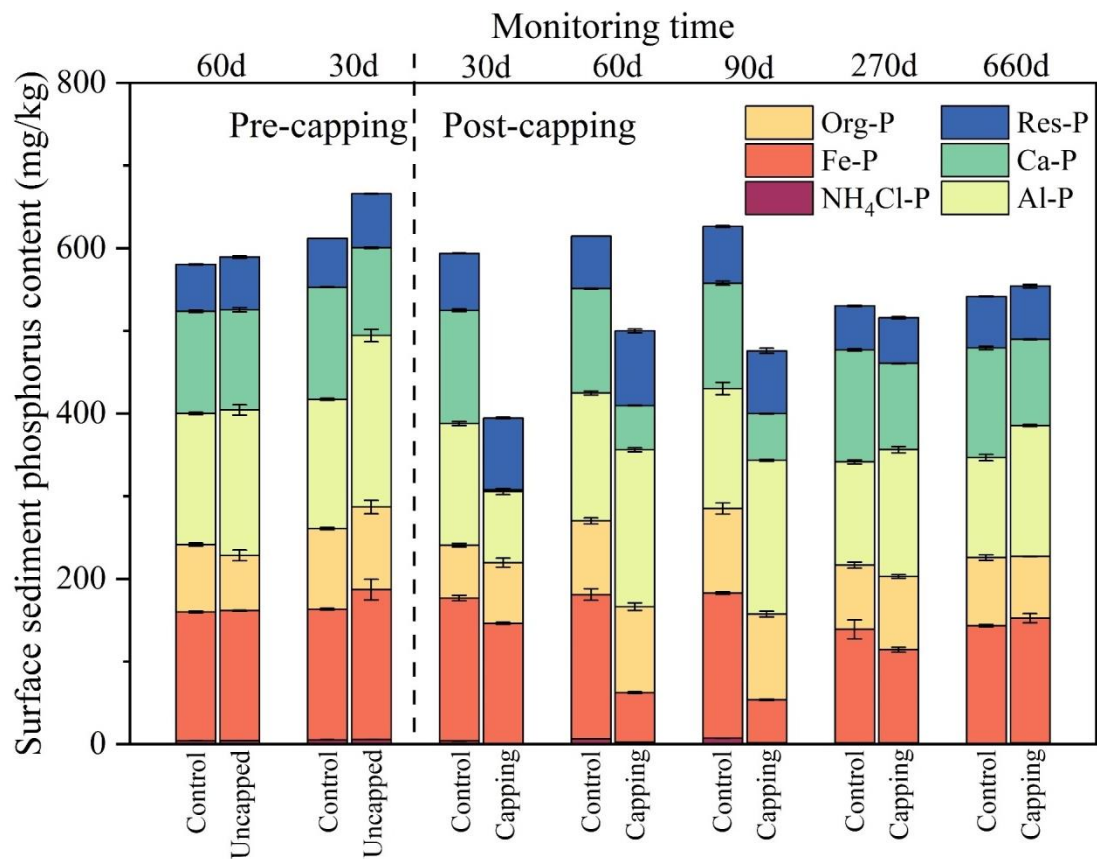
**Fig. 1.** Location of the field enclosure and the sampling sites in Lake Taihu.





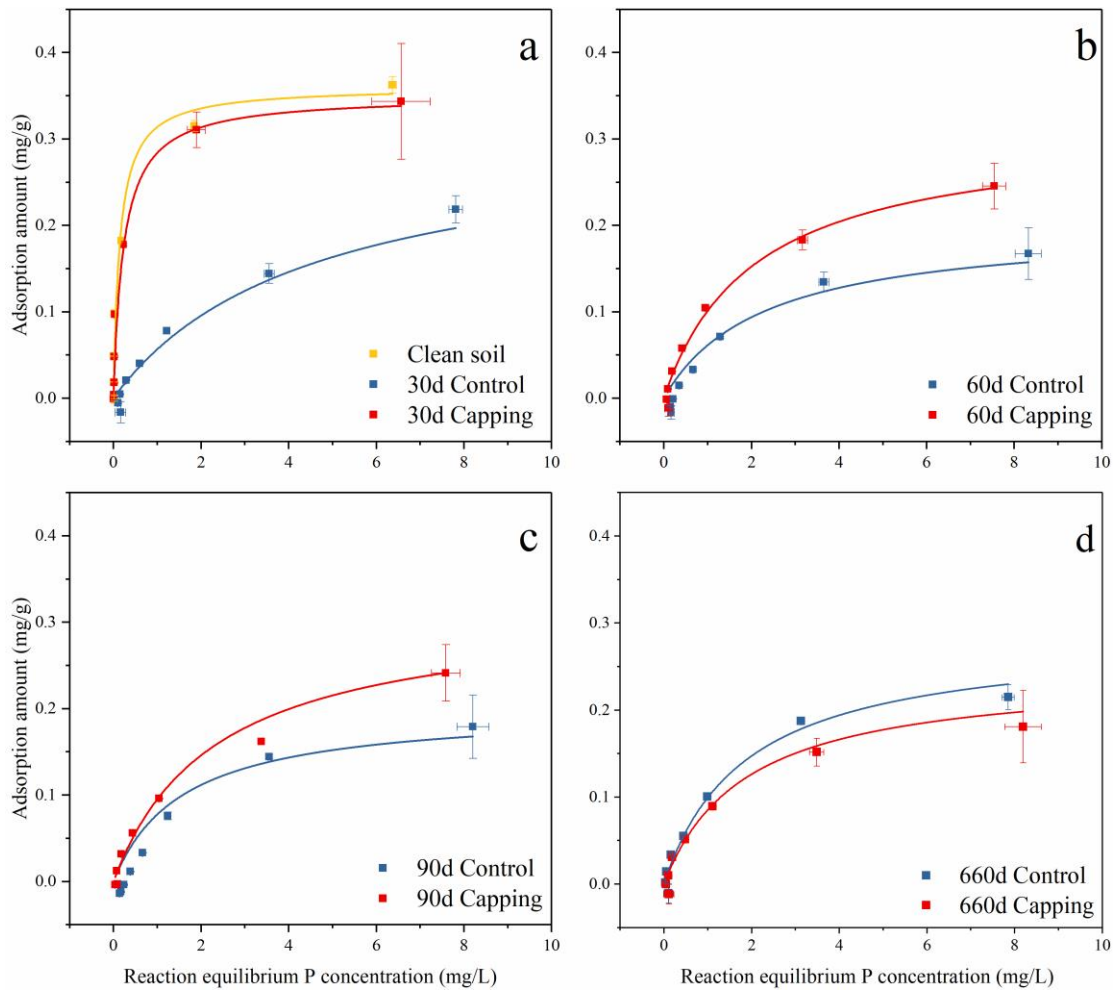
660  
 661  
 662  
 663  
 664

**Fig. 2.** TN and DIN in control and capping sediment treatment at seven sampling times.



665  
666  
667  
668

**Fig. 3.** TP and P fractions in control and capping sediment at seven sampling times.



670

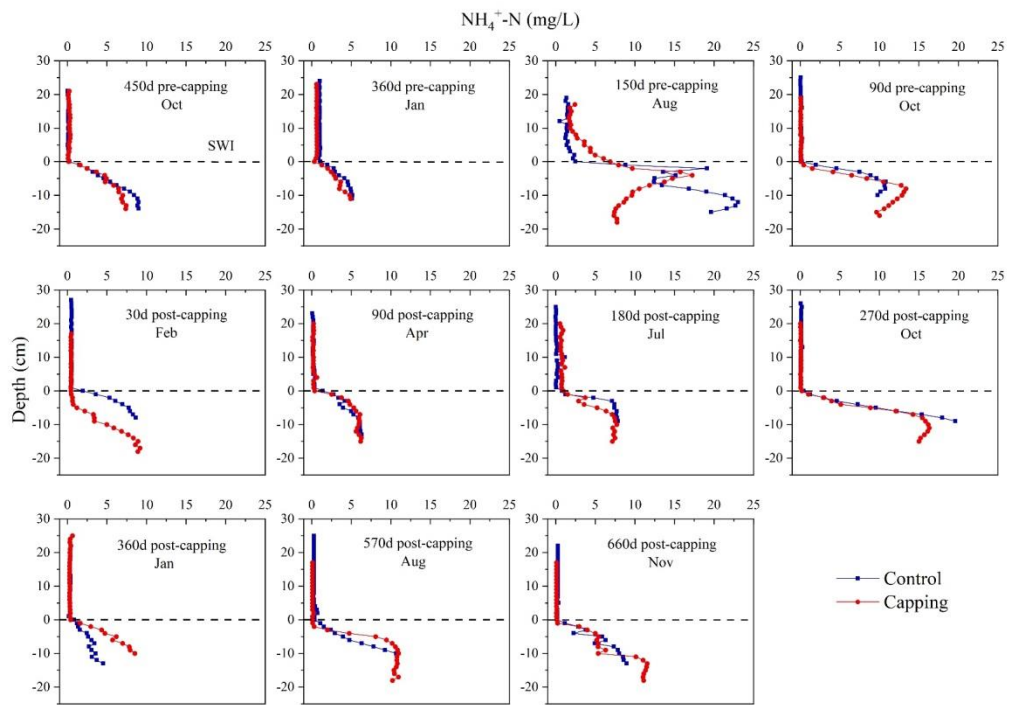
671

**Fig. 4.** Phosphorus adsorption isotherm regression for clean soil, control and capping sediment treatment using the non-linear form of the Langmuir equation.

672

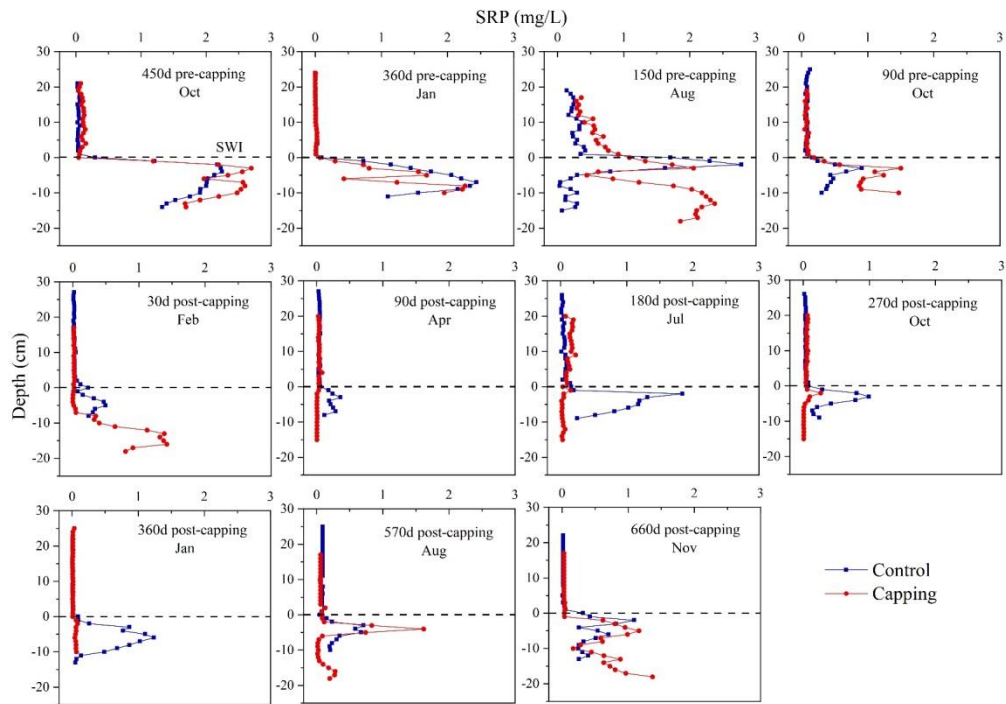
673

674



675  
 676  
 677

**Fig. 5.**  $\text{NH}_4^+\text{-N}$  concentration in porewater profiles for control and capping sediment at eleven sampling times.



679

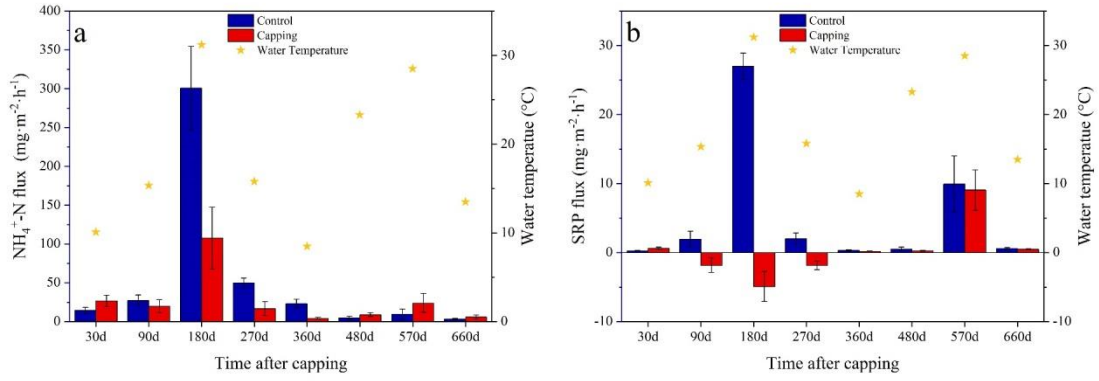
680

**Fig. 6.** SRP concentration in porewater profiles for control and capping sediment at eleven sampling times.

681

682

683



684

685

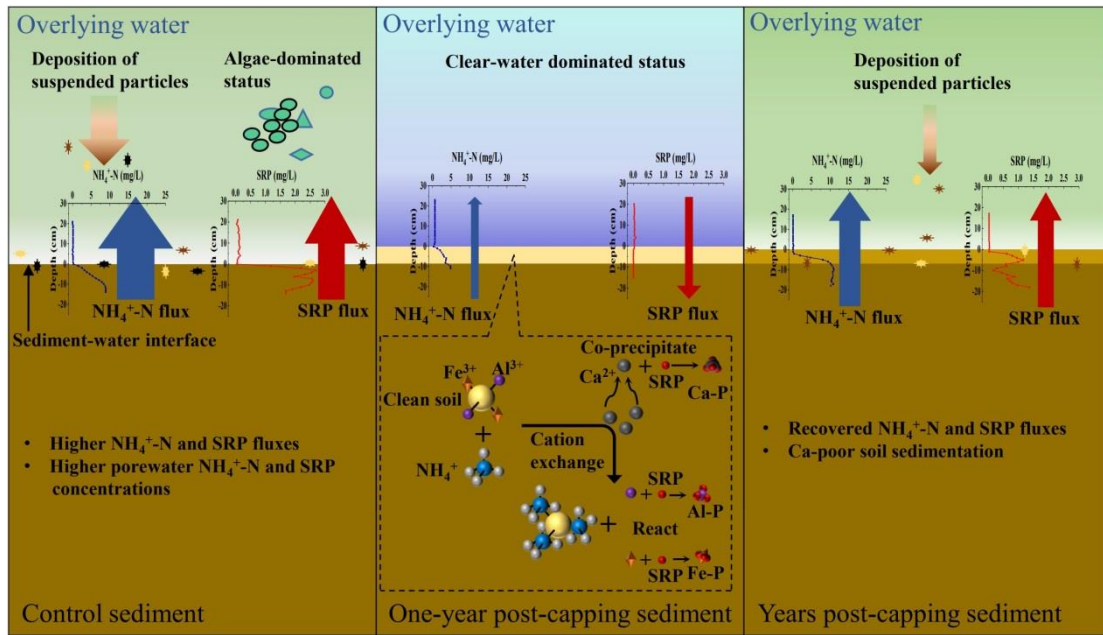
**Fig. 7.** Diffusive fluxes of NH<sub>4</sub><sup>+</sup>-N and SRP across the sediment-water interface for control and capping sediment at eight sampling times.

686

687

688

689



690

691 **Fig. 8.** Schematic representation of Ca-poor soil capping in control sediment internal  
 692 loading, and the response of overlying water status in temporally.

693

694

695

696 **References**

- 697 Ajmal, Z., Muhmood, A., Usman, M., Kizito, S., Lu, J., Dong, R., Wu, S., 2018.  
698 Phosphate removal from aqueous solution using iron oxides: Adsorption,  
699 desorption and regeneration characteristics. *J. Colloid Interface Sci.* 528, 145–  
700 155.
- 701 Alshameri, A., Ibrahim, A., Assabri, A.M., Lei, X., Wang, H., Yan, C., 2014. The  
702 investigation into the ammonium removal performance of Yemeni natural  
703 zeolite: Modification, ion exchange mechanism, and thermodynamics. *Powder*  
704 *Technol.* 258, 20–31.
- 705 Beutel, M.W., 2006. Inhibition of ammonia release from anoxic profundal sediments  
706 in lakes using hypolimnetic oxygenation. *Ecol. Eng.* 28(3), 271–279.
- 707 Blindow, I., 1992. Long- and short-term dynamics of submerged macrophytes in two  
708 shallow eutrophic lakes. *Freshwater Biol.* 28(1), 15–27.
- 709 Bullerjahn, G.S., McKay, R.M., Davis, T.W., Baker, D.B., Boyer, G.L., D'Anglada,  
710 L.V., Doucette, G.J., Ho, J.C., Irwin, E.G., Kling, C.L., Kudela, R.M.,  
711 Kurmayer, R., Michalak, A.M., Ortiz, J.D., Otten, T.G., Paerl, H.W., Qin, B.,  
712 Sohngen, B.L., Stumpf, R.P., Visser, P.M., Wilhelm, S.W., 2016. Global  
713 solutions to regional problems: Collecting global expertise to address the  
714 problem of harmful cyanobacterial blooms. A Lake Erie case study. *Harmful*  
715 *Algae* 54, 223–238.
- 716 Cao, D., Jin, X., Gan, L., Wang, T., Chen, Z., 2016. Removal of phosphate using  
717 iron oxide nanoparticles synthesized by eucalyptus leaf extract in the presence  
718 of CTAB surfactant. *Chemosphere* 159, 23–31.
- 719 Chen, M., Ding, S., Liu, L., Xu, D., Han, C., Zhang, C., 2015. Iron-coupled  
720 inactivation of phosphorus in sediments by macrozoobenthos (chironomid  
721 larvae) bioturbation: Evidences from high-resolution dynamic measurements.  
722 *Environ. Pollut.* 204, 241–247.
- 723 Chinese EPA, 2002. *Methods for the Examination of Water and Wastewater*. China  
724 Environmental Science Press: Beijing, China, 243–258.
- 725 Copetti, D., Finsterle, K., Marziali, L., Stefani, F., Tartari, G., Douglas, G., Reitzel,  
726 K., Spears, B.M., Winfield, I.J., Crosa, G., D'Haese, P., Yasserli, S., Lürling,  
727 M., 2016. Eutrophication management in surface waters using lanthanum  
728 modified bentonite: A review. *Water Res.* 97, 162–174.
- 729 Cotner, J.B., 2017. Nitrogen is Not a 'House of Cards'. *Environ. Sci. Technol.* 51(1),  
730 3–3.
- 731 Ding, S., Chen, M., Gong, M., Fan, X., Qin, B., Xu, H., Gao, S., Jin, Z., Tsang,  
732 D.C.W., Zhang, C., 2018. Internal phosphorus loading from sediments causes  
733 seasonal nitrogen limitation for harmful algal blooms. *Sci. Total Environ.* 625,  
734 872–884.
- 735 Figueiredo, C., Grilo, T.F., Oliveira, R., Ferreira, I.J., Gil, F., Lopes, C., Brito, P.,  
736 Ré, P., Caetano, M., Diniz, M., Raimundo, J., 2022. Single and combined  
737 ecotoxicological effects of ocean warming, acidification and lanthanum  
738 exposure on the surf clam (*Spisula solida*). *Chemosphere* 302, 134850.
- 739 Gan, B.K., Madsen, I.C., Hockridge, J.G., 2009. In situ X-ray diffraction of the



740 transformation of gibbsite to  $\alpha$ -alumina through calcination: effect of particle  
741 size and heating rate. *J. Appl. Crystallogr.* 42(4), 697–705.

742 Gibbs, M.M., Hickey, C.W., 2018. Flocculants and Sediment Capping for  
743 Phosphorus management. In *Lake Restoration Handbook*. Springer, Cham, pp.  
744 207–265.

745 Gu, B.W., Hong, S.H., Lee, C.G., Park, S.J., 2019. The feasibility of using bentonite,  
746 illite, and zeolite as capping materials to stabilize nutrients and interrupt their  
747 release from contaminated lake sediments. *Chemosphere* 219, 217–226.

748 Gu, B.W., Lee, C.G., Lee, T.G., Park, S.J., 2017. Evaluation of sediment capping  
749 with activated carbon and nonwoven fabric mat to interrupt nutrient release  
750 from lake sediments. *Sci. Total Environ.* 599-600, 413–421.

751 Guo, L., 2007. Ecology - Doing battle with the green monster of Taihu Lake.  
752 *Science*. 317(5842), 1166–1166.

753 Hinsinger, P., 2001. Bioavailability of soil inorganic P in the rhizosphere as  
754 affected by root-induced chemical changes: a review. *Plant soil* 237(2), 173–  
755 195.

756 Huser, B.J., Egemose, S., Harper, H., Hupfer, M., Jensen, H., Pilgrim, K.M., Reitzel,  
757 K., Rydin, E., Futter, M., 2016. Longevity and effectiveness of aluminum  
758 addition to reduce sediment phosphorus release and restore lake water quality.  
759 *Water Res.* 97, 122–132.

760 Lai, D.Y.F., Lam, K.C., 2009. Phosphorus sorption by sediments in a subtropical  
761 constructed wetland receiving stormwater runoff. *Ecol. Eng.* 35(5), 735–743.

762 Leyva-Ramos, R., Jacobo-Azuara, A., Diaz-Flores, P.E., Guerrero-Coronado, R.M.,  
763 Mendoza-Barron, J., Berber-Mendoza, M.S., 2008. Adsorption of chromium  
764 (VI) from an aqueous solution on a surfactant-modified zeolite. *Colloids Surf.,*  
765 *A* 330(1), 35–41.

766 Li, X., Xie, Q., Chen, S., Xing, M., Guan, T., Wu, D., 2019. Inactivation of  
767 phosphorus in the sediment of the Lake Taihu by lanthanum modified zeolite  
768 using laboratory studies. *Environ. Pollut.* 247, 9–17.

769 Li, Y., Fan, Y., Li, X., Wu, D., 2017. Evaluation of zeolite/hydrous aluminum oxide  
770 as a sediment capping agent to reduce nutrients level in a pond. *Ecol. Eng.* 101,  
771 170–178.

772 Lin, J., He, S., Zhang, H., Zhan, Y., Zhang, Z., 2019. Effect of zirconium-modified  
773 zeolite addition on phosphorus mobilization in sediments. *Sci. Total Environ.*  
774 646, 144–157.

775 Lin, J., Zhan, Y., Zhu, Z., 2011. Evaluation of sediment capping with active barrier  
776 systems (ABS) using calcite/zeolite mixtures to simultaneously manage  
777 phosphorus and ammonium release. *Sci. Total Environ.* 409(3), 638–646.

778 Lin, L., Lei, Z., Wang, L., Liu, X., Zhang, Y., Wan, C., Lee, D.-J., Tay, J.H., 2013.  
779 Adsorption mechanisms of high-levels of ammonium onto natural and  
780 NaCl-modified zeolites. *Sep. Purif. Technol.* 103, 15–20.

781 Lin, L., Wan, C., Lee, D.-J., Lei, Z., Liu, X., 2014. Ammonium assists  
782 orthophosphate removal from high-strength wastewaters by natural zeolite. *Sep.*  
783 *Purif. Technol.* 133, 351–356.

- 784 Liu, C., Du, Y., Yin, H., Fan, C., Chen, K., Zhong, J., Gu, X., 2019. Exchanges of  
785 nitrogen and phosphorus across the sediment-water interface influenced by the  
786 external suspended particulate matter and the residual matter after dredging.  
787 *Environ. Pollut.* 246, 207–216.
- 788 Liu, C., Du, Y., Zhong, J., Zhang, L., Huang, W., Han, C., Chen, K., Gu, X., 2022.  
789 From macrophyte to algae: Differentiated dominant processes for internal  
790 phosphorus release induced by suspended particulate matter deposition. *Water*  
791 *Res.* 224, 119067.
- 792 Liu, C., Zhong, J., Wang, J., Zhang, L., Fan, C., 2016. Fifteen-year study of  
793 environmental dredging effect on variation of nitrogen and phosphorus  
794 exchange across the sediment-water interface of an urban lake. *Environ. Pollut.*  
795 219, 639–648.
- 796 Lurling, M., Mackay, E., Reitzel, K., Spears, B.M., 2016. Editorial - A critical  
797 perspective on geo-engineering for eutrophication management in lakes. *Water*  
798 *Res.* 97, 1–10.
- 799 Moore, B.C., Lafer, J.E., Funk, W.H., 1994. Influence of aquatic macrophytes on  
800 phosphorus and sediment porewater chemistry in a freshwater wetland. *Aquat.*  
801 *Bot.* 49(2–3), 137–148.
- 802 Paerl, H.W., Scott, J.T., McCarthy, M.J., Newell, S.E., Gardner, W.S., Havens, K.E.,  
803 Hoffman, D.K., Wilhelm, S.W., Wurtsbaugh, W.A., 2016. It Takes Two to  
804 Tango: When and Where Dual Nutrient (N & P) Reductions Are Needed to  
805 Protect Lakes and Downstream Ecosystems. *Environ. Sci. Technol.* 50(20),  
806 10805–10813.
- 807 Pan, G., Dai, L., Li, L., He, L., Li, H., Bi, L., Gulati, R.D., 2012a. Reducing the  
808 Recruitment of Sedimented Algae and Nutrient Release into the Overlying  
809 Water Using Modified Soil/Sand Flocculation-Capping in Eutrophic Lakes.  
810 *Environ. Sci. Technol.* 46(9), 5077–5084.
- 811 Pan, G., Dai, L., Li, L., Shang, Y., Li, H., Bi, L., He, L., Wang, L., Wang, D., Li, Q.,  
812 Li, L., Gu, X., Zhong, J., Yu, Y., Yan, Q., 2012b. Eutrophication control using  
813 modified local soil/sand induced ecological restoration technology: I. Effect  
814 and mechanism on short and long term improvement of water quality. *Sci.*  
815 *Limnol. Sin.* 24(6), 801–810.
- 816 Pan, G., Krom, M.D., Zhang, M., Zhang, X., Wang, L., Dai, L., Sheng, Y., Mortimer,  
817 R.J.G., 2013. Impact of suspended inorganic particles on phosphorus cycling in  
818 the Yellow River (China). *Environ. Sci. Technol.* 47 (17), 9685–9692.
- 819 Pan, G., Miao, X., Bi, L., Zhang, H., Wang, L., Wang, L., Wang, Z., Chen, J., Ali, J.,  
820 Pan, M., Zhang, J., Yue, B., Lyu, T., 2019. Modified Local Soil (MLS)  
821 Technology for Harmful Algal Bloom Control, Sediment Remediation, and  
822 Ecological Restoration. *Water* 11(6), 1123.
- 823 Pan, G., Krom, M. D., Herut, B., 2002. Adsorption-Desorption of Phosphate on  
824 Airborne Dust and Riverborne Particulates in East Mediterranean Seawater.  
825 *Environ. Sci. Technol.* 36(16), 3519–3524.
- 826 Peterson, S.A., Sanville, W.D., Stay, F.S., Powers, C.F., 1976. Laboratory  
827 evaluation of nutrient inactivation compounds for lake restoration. *J. Water*

828 Pollut. Control Fed., 817–831.

829 Qin, B., Xu, P., Wu, Q., Luo, L. Zhang, Y., 2007. Environmental Issues of Lake  
830 Taihu, China. In *Eutrophication of shallow lakes with special reference to Lake*  
831 *Taihu, China*. Springer, Dordrecht, pp. 3–14.

832 Roberts, K.L., Eate, V.M., Eyre, B.D., Holland, D.P., Cook, P.L.M., 2012. Hypoxic  
833 events stimulate nitrogen recycling in a shallow salt-wedge estuary: The Yarra  
834 River estuary, Australia. *Limnol. Oceanogr.* 57(5), 1427–1442.

835 Rönicke, H., Frassl, M.A., Rinke, K., Tittel, J., Beyer, M., Kormann, B., Gohr, F.,  
836 Schultze, M., 2021. Suppression of bloom-forming colonial cyanobacteria by  
837 phosphate precipitation: A 30 years case study in Lake Barleber (Germany).  
838 *Ecol. Eng.* 162, 106171.

839 Rukun, L., 1999. *Analytical methods for soil and agricultural chemistry*.  
840 *Agricultural Science and Technology Press of China: Beijing*, pp. 15–20.

841 Rydin, E., 2000. Potentially mobile phosphorus in Lake Erken sediment. *Water Res.*  
842 34(7), 2037–2042.

843 Sand-Jensen, K., Martinsen, K.T., Jakobsen, A.L., Sjø, J.S., Madsen-Østerbye, M.,  
844 Kjær, J.E., Kristensen, E., Kragh, T., 2021. Large pools and fluxes of carbon,  
845 calcium and phosphorus in dense charophyte stands in ponds. *Sci. Total*  
846 *Environ.* 765, 142792.

847 Scheffer, M., van Nes, E.H., 2007. Shallow lakes theory revisited: various  
848 alternative regimes driven by climate, nutrients, depth and lake size.  
849 *Hydrobiologia* 584 (1), 455–466.

850 Schnürer, J., Rosswall, T., 1982. Fluorescein diacetate hydrolysis as measure of  
851 total microbial activity in soil and litter. *Appl. Environ. Microb.* 43(6), 1256–  
852 1256.

853 Shannon, K.E.M., Saleh-Lakha, S., Burton, D.L., Zebarth, B.J., Goyer, C., Trevors,  
854 J.T., 2011. Effect of nitrate and glucose addition on denitrification and nitric  
855 oxide reductase (cnorB) gene abundance and mRNA levels in *Pseudomonas*  
856 *mandelii* inoculated into anoxic soil. *Antonie van Leeuwenhoek.* 100(2), 183–  
857 195.

858 Spears, B.M., Maberly, S.C., Pan, G., Mackay, E., Bruere, A., Corker, N., Douglas,  
859 G., Egemose, S., Hamilton, D., Hatton-Ellis, T., Huser, B., Li, W., Meis, S.,  
860 Moss, B., Lurling, M., Phillips, G., Yasserli, S., Reitzel, K., 2014.  
861 Geo-engineering in lakes: a crisis of confidence? *Environ. Sci. Technol.* 48(17),  
862 9977–9979.

863 Sun, C., Wang, S., Wang, H., Hu, X., Yang, F., Tang, M., Zhang, M., Zhong, J.,  
864 2022. Internal nitrogen and phosphorus loading in a seasonally stratified  
865 reservoir: Implications for eutrophication management of deep-water  
866 ecosystems. *J. Environ. Manage.* 319, 115681.

867 Sun, S., Huang, S., Sun, X., Wen, W., 2009. Phosphorus fractions and its release in  
868 the sediments of Haihe River, China. *J. Environ. Sci.* 21(3), 291–295.

869 Tammeorg, O., Nürnberg, G., Horppila, J., Haldna, M., Niemistö, J., 2020.  
870 Redox-related release of phosphorus from sediments in large and shallow Lake  
871 Peipsi: Evidence from sediment studies and long-term monitoring data. *J. Great*

872 Lakes Res. 46(6), 1595–1603.

873 Wang, J., Chen, J., Ding, S., Guo, J., Christopher, D., Dai, Z., Yang, H., 2016.

874 Effects of seasonal hypoxia on the release of phosphorus from sediments in

875 deep-water ecosystem: A case study in Hongfeng Reservoir, Southwest China.

876 Environ. Pollut. 219, 858–865.

877 Wang, Y., Ding, S., Wang, D., Sun, Q., Lin, J., Shi, L., Chen, M., Zhang, C., 2017.

878 Static layer: A key to immobilization of phosphorus in sediments amended with

879 lanthanum modified bentonite (Phoslock®). Chem. Eng. J. 325, 49–58.

880 Watson, S.B., Miller, C., Arhonditsis, G., Boyer, G.L., Carmichael, W., Charlton,

881 M.N., Confesor, R., Depew, D.C., Höök, T.O., Ludsin, S.A., Matisoff, G.,

882 McElmurry, S.P., Murray, M.W., Peter Richards, R., Rao, Y.R., Steffen, M.M.,

883 Wilhelm, S.W., 2016. The re-eutrophication of Lake Erie: Harmful algal

884 blooms and hypoxia. Harmful Algae 56, 44–66.

885 Wen, S., Zhong, J., Li, X., Liu, C., Yin, H., Li, D., Ding, S., Fan, C., 2020. Does

886 external phosphorus loading diminish the effect of sediment dredging on

887 internal phosphorus loading? An in-situ simulation study. J. Hazard. Mater. 394,

888 122548.

889 Wu, Z., Wang, C., Jiang, H., Li, K., Yang, X., Huang, W., 2022. Sediment pH

890 structures the potential of the lake's internal P pollution involved in different

891 types of P reactivation. J. Cleaner Prod. 352, 131576.

892 Xu, R., Zhang, M., Mortimer, R.J.G., Pan, G., 2017. Enhanced Phosphorus Locking

893 by Novel Lanthanum/Aluminum–Hydroxide Composite: Implications for

894 Eutrophication Control. Environ. Sci. Technol. 51(6), 3418–3425.

895 Yang, C., Yang, P., Geng, J., Yin, H., Chen, K., 2020. Sediment internal nutrient

896 loading in the most polluted area of a shallow eutrophic lake (Lake Chaohu,

897 China) and its contribution to lake eutrophication. Environ. Pollut. 262,

898 114292.

899 Yin, H., Yang, C., Yang, P., Kaksonen, A.H., Douglas, G.B., 2021. Contrasting

900 effects and mode of dredging and in situ adsorbent amendment for the control

901 of sediment internal phosphorus loading in eutrophic lakes. Water Res. 189,

902 116644.

903 Yu, J., Ding, S., Zhong, J., Fan, C., Chen, Q., Yin, H., Zhang, L., Zhang, Y., 2017.

904 Evaluation of simulated dredging to control internal phosphorus release from

905 sediments: Focused on phosphorus transfer and resupply across the

906 sediment-water interface. Sci. Total Environ. 592, 662–673.

907 Zhan, Y., Yu, Y., Lin, J., Wu, X., Wang, Y., Zhao, Y., 2019. Simultaneous control

908 of nitrogen and phosphorus release from sediments using iron-modified zeolite

909 as capping and amendment materials. J. Environ. Manage. 249, 109369.

910 Zhang, H., Lyu, T., Liu, L., Hu, Z., Chen, J., Su, B., Yu, J., Pan, G., 2021. Exploring

911 a multifunctional geoengineering material for eutrophication remediation:

912 Simultaneously control internal nutrient load and tackle hypoxia. Chem. Eng. J.

913 406, 127206.

914 Zhong, J.C., Yu, J.H., Zheng, X.L., Wen, S.L., Liu, D.H., Fan, C.X., 2018. Effects

915 of Dredging Season on Sediment Properties and Nutrient Fluxes across the

916 Sediment–Water Interface in Meiliang Bay of Lake Taihu, China. *Water* 10(11),  
917 1606.

918 Zhong, J., Chen, C., Yu, J., Shen, Q., Liu, C., Fan, C., 2022. Effect of dredging and  
919 capping with clean soil on the mitigation of algae-induced black blooms in  
920 Lake Taihu, China: A simulation study. *J. Environ. Manage.* 302, 114106.

921 Zhong, J., Fan, C., Liu, G., Zhang, L., Shang, J., Gu, X., 2010a. Seasonal variation  
922 of potential denitrification rates of surface sediment from Meiliang Bay, Taihu  
923 Lake, China. *J. Environ. Sci.* 22(7), 961–967.

924 Zhong, J., Fan, C., Zhang, L., Hall, E., Ding, S., Li, B., Liu, G., 2010b. Significance  
925 of dredging on sediment denitrification in Meiliang Bay, China: A year-long  
926 simulation study. *J. Environ. Sci.* 22(1), 68–75.

927 Zhong, J., Wen, S., Zhang, L., Wang, J., Liu, C., Yu, J., Zhang, L., Fan, C., 2021.  
928 Nitrogen budget at sediment–water interface altered by sediment dredging and  
929 settling particles: Benefits and drawbacks in managing eutrophication. *J.*  
930 *Hazard. Mater.* 406, 124691.

931 Zhou, J., Li, D., Chen, S., Xu, Y., Geng, X., Guo, C., Huang, Y., 2019. Sedimentary  
932 phosphorus immobilization with the addition of amended calcium peroxide  
933 material. *Chem. Eng. J.* 357, 288–297.

934

935